Applied Mathematics and Computation 248 (2014) 93–100

Contents lists available at ScienceDirect

Applied Mathematics and Computation

journal homepage: www.elsevier.com/locate/amc

The singular function boundary integral method for an elastic plane stress wedge beam problem with a point boundary singularity

Miltiades C. Elliotis [a,*], Dimos C. Charmpis [b], Georgios C. Georgiou [a]

[a] Department of Mathematics and Statistics, University of Cyprus, 75 Kallipoleos Str., P.O. Box 20537, 1678 Nicosia, Cyprus
[b] Department of Civil and Environmental Engineering, University of Cyprus, 75 Kallipoleos Str., P.O. Box 20537, 1678 Nicosia, Cyprus

A R T I C L E I N F O

Keywords:
Laplace equation
Point boundary singularity
Singular function boundary integral method
Lagrange multipliers
Singular functions
Singular coefficients

A B S T R A C T

The singular function boundary integral method (SFBIM) is applied for the numerical solution of a 2-D Laplace model problem of a perfectly elastic wedge beam under plane stress conditions. The beam has a point boundary singularity, it includes a curved boundary part and is subjected to non-trivial distributed external loading. The implemented solution method converges for this special model problem extremely fast. The numerical estimates attained for the leading singular coefficients of the local asymptotic expansion and the stress and strain fields are highly accurate, as verified by comparison with the available analytical solution.

1. Introduction

In the area of linear elasticity, there exist many problems described by the Laplace equation in either two or three dimensions. When boundary singularities are present, caused either by an abrupt change in the boundary conditions or by a re-entrant corner, one needs to compute the singular coefficients of the solution expansion in the neighborhood of the singularity, which is intended to represent the Airy stress function Φ. In the case of a plane problem in polar coordinates, this expansion is of the form:

$$\Phi(r,\theta) = \sum_{j=1}^{\infty} \beta_j r^{\lambda_j} f_j(\theta), \tag{1}$$

where the polar coordinates (r, θ) are centered at the singular point. The eigenvalues λ_j and the eigenfunctions f_j of the problem are determined by the boundary conditions along the boundary parts causing the singularity. The values of the unknown singular coefficients β_j, determined by the boundary conditions at the rest of the boundary, are of significant importance in many applications. In fracture mechanics these coefficients are also known as generalized stress intensity factors [1].

In the past few decades, many special numerical methods have been proposed for the solution of elliptic boundary value problems with boundary singularities, in order to overcome difficulties related to the lack of adequate accuracy and to poor convergence in the neighborhood of singularity points. Remedies used were special mesh refinement schemes, multigrid methods, singular elements, *p*/*hp* finite elements and many other techniques (see, e.g. [2–5]). An extensive survey of the treatment of singularities in elliptic boundary value problems is provided in the review article by Li and Lu [6].

* Corresponding author.
E-mail address: m-elliotis@live.com (M.C. Elliotis).

http://dx.doi.org/10.1016/j.amc.2014.09.090

Certain techniques incorporate the form of the local asymptotic expansion [7]. For example, Georgiou and co-workers [8,9] developed a singular finite element method, in which special elements are employed. With their method, the radial form of the local singularity expansion is employed, in the neighborhood of the singularity, in order to resolve the convergence difficulties and improve the accuracy of the global solution. In the Finite Element Method (FEM), the singular coefficients are calculated by post-processing of the numerical solution. Especially with high-order *p* and *hp* FEM versions, fast convergence is achieved by: (i) increasing the degree of the piecewise polynomials (in the case of the *p* version) and (ii) by decreasing the characteristic size *h* of the elements and increasing *p* (in the case of the *hp* version). Such methods proved very successful in solving elliptic boundary value problems with a boundary singularity [10,11]. Also, some interesting post-processing procedures have been proposed for the calculation of the singular coefficients from the finite element solution [3,4].

In the past two decades, Georgiou and co-workers [12–18] developed and tested the Singular Function Boundary Integral Method (SFBIM), in which the unknown singular coefficients are calculated directly, thus giving directly the approximation of the Airy stress function in Laplacian and biharmonic problems of plane elasticity, or the stream-function in biharmonic problems of fluid mechanics. Recently, an extension of the method has been made for 3-D elliptic problems of elasticity [17]. With the SFBIM the solution is approximated by the leading terms of expansion (1) and the Dirichlet conditions on boundary parts away from the singularity are enforced by means of Lagrange multipliers. Numerical studies, as well as theoretical analyses, demonstrated that the SFBIM exhibits exponential convergence with the number of singular functions and can achieve high solution accuracy [12–18].

In the present work, the SFBIM is applied for the solution of a 2-D Laplace model problem of a perfectly elastic wedge beam under plane stress conditions. The beam has a curved boundary part, the center of curvature of which does not coincide with the point of boundary singularity. The distributed external loads applied to the beam impose non-standard boundary conditions, which would be difficult to handle in the framework of the classical FEM or other approaches. The analytical expression of the Airy stress function for this problem is known, which allows for objective accuracy assessment of the implemented numerical method. Hence, our objectives are: (a) to efficiently solve this special model problem without transforming it into an equivalent biharmonic problem (with the angle of the wedge being less than $3\pi/4$, it is impossible to find a real function for the local solution expansion); and (b) to study the convergence and the accuracy of the SFBIM. The model problem is described in Section 2. In Section 3, the formulation of the SFBIM is presented. Section 4 reports and discusses the numerical results obtained and demonstrates the fast convergence of the SFBIM. Finally, the conclusions are summarized in Section 5.

2. A model problem with a point boundary singularity

We consider the plane stress problem of the 2-D unit-thickness wedge beam schematically illustrated in Fig. 1. The beam has two free straight boundary parts, which are subjected to distributed normal and shear loads, as well as a supported curved boundary part. More specifically, distributed normal pressures $p(r)$ act vertically and horizontally along the boundary segment OA of length L, while a distributed shear load $\tau(r)$ acts along the inclined boundary segment OB. External loading consists of these distributed loads only; there are no concentrated external forces on the structure. Moreover, the self-weight of the beam is ignored. The third boundary segment AB, which is fixed-supported and curved, is part of the circumference of a circle with center at point K and radius R; the y-coordinate of K is equal to $H/2$, which is half the length of chord AB. The singularity of this problem is at the free tip O of the wedge, which lies at the intersection of the two straight loaded boundary segments OA and OB. The center K of the circle defining the curved boundary part AB is far away from the singular point O.

The physical boundary conditions of this model problem are as follows:

$$\left.\begin{array}{ll} \sigma_{rr} = -p(r) = -3r - 0.01r^7, \quad \sigma_{\theta\theta} = p(r) = -\sigma_{rr}, \quad \sigma_{r\theta} = 0 & \text{on} \quad \mathrm{OA} \\ \sigma_{rr} = \sigma_{\theta\theta} = 0, \quad \sigma_{r\theta} = \tau(r) = 3r - 0.01r^7 & \text{on} \quad \mathrm{OB} \\ u_r = u_\theta = 0 & \text{on} \quad \mathrm{AB} \end{array}\right\}, \tag{2}$$

where the stresses σ_{rr}, $\sigma_{\theta\theta}$ and $\sigma_{r\theta}$ and the displacements u_r and u_θ can easily be deduced from $\Phi(r,\theta)$ expressed in polar coordinates. Note that all expressions are dimensional; distributed loads are expressed in kN/m and lengths in m (L = 3 m, R = 10 m). Fig. 2 gives a graphical presentation of the distributed loads $p(r)$ and $\tau(r)$ acting along boundaries OA and OB, respectively, in order to provide a view of the non-trivial loading conditions of the structure analyzed. The material

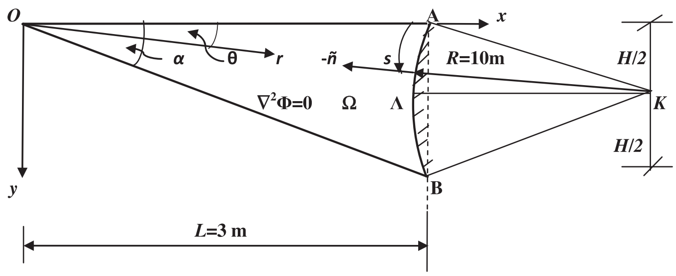

Fig. 1. Schematic illustration of the 2-D wedge beam.

of the wedge beam is assumed to exhibit perfectly elastic behavior; the structure is made of a typical aluminum alloy with Young's modulus $E = 70$ GPa and Poisson's ratio $\nu = 1/3$. The type of problem studied in the present paper is of interest in engineering applications [19].

With the wedge angle being $\alpha = \pi/6$, the corresponding eigensolutions are

$$\lambda_j = 3(2j-1), \quad f_j(\theta) = \cos(\lambda_j\theta), \quad j = 1, 2, \ldots \tag{3}$$

Hence, the local solution reads

$$\Phi(r,\theta) = \sum_{j=1}^{\infty} \beta_j Q_j, \tag{4}$$

where

$$Q_j = r^{\lambda_j} \cos(\lambda_j\theta) \tag{5}$$

are known as the singular functions. With the particular choice of the boundary condition along AB, it turns out that only the first two singular coefficients are non-zero: $\beta_1 = 1/2$ and $\beta_2 = 1/7200$. In other words,

$$\Phi(r,\theta) = \frac{1}{2} r^3 \cos(3\theta) + \frac{1}{7200} r^9 \cos(9\theta). \tag{6}$$

According to Kirchhoff's uniqueness theorem, the above solution is unique [19].

In terms of Φ, the mathematical problem to be solved is the following:

$$\nabla^2\Phi = 0 \quad \text{in} \quad \Omega \tag{7}$$

subject to the following boundary conditions:

$$\left.\begin{array}{l} \dfrac{\partial\Phi}{\partial\theta} = 0 \quad \text{on} \quad \mathrm{OA} \\ \Phi = 0 \quad \text{on} \quad \mathrm{OB} \\ \Phi = \frac{1}{2} r^3 \cos(3\theta) + \frac{1}{7200} r^9 \cos(9\theta) \quad \text{on} \quad \mathrm{AB} \end{array}\right\}. \tag{8}$$

3. The singular function boundary integral method

With the SFBIM, the solution of the model problem analyzed is approximated by the leading N_s terms of the local asymptotic expansion (4):

$$\bar{\Phi}(r,\theta) = \sum_{j=1}^{N_s} \bar{\beta}_j Q_j, \tag{9}$$

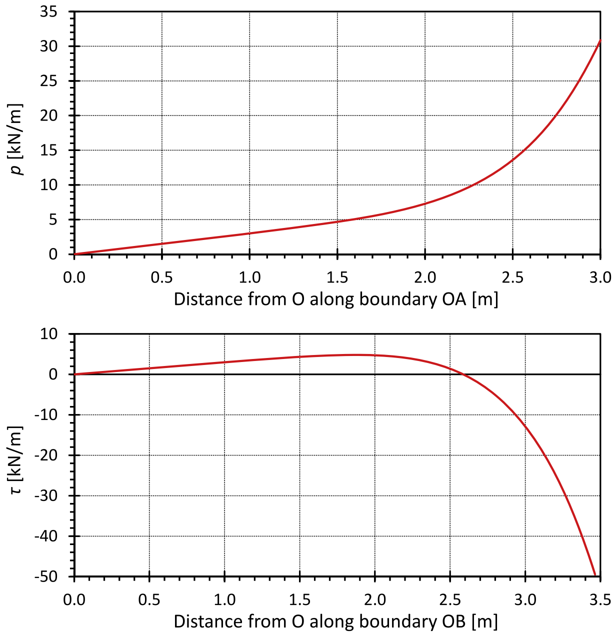

Fig. 2. Graphical presentation of the distributions of the normal load $p(r)$ and the shear load $\tau(r)$ acting along boundary parts OA and OB, respectively.

where the overbars denote approximate quantities. The governing equation (7) is weighted, in the Galerkin sense, by the singular functions Q_i and integration is performed over the whole domain Ω. Hence, the discretized problem reads

$$\int_{\Omega} Q_i \nabla^2 \bar{\Phi} \mathrm{d}V = 0, \quad i = 1, 2, \ldots, N_s. \tag{10}$$

By applying Green's second identity, the dimension of the problem is reduced by one:

$$\int_{\partial\Omega} \left(Q_i \frac{\partial \bar{\Phi}}{\partial n} - \bar{\Phi} \frac{\partial Q_i}{\partial n} \right) \mathrm{d}s = 0, \quad i = 1, 2, \ldots, N_s, \tag{11}$$

where n denotes the direction normal to the boundary. Since the singular functions Q_i satisfy the corresponding boundary conditions, the above integral is zero along OA and OB. Therefore, one needs to integrate only far from the singularity:

$$\int_{\mathrm{AB}} \left(Q_i \frac{\partial \bar{\Phi}}{\partial n} - \bar{\Phi} \frac{\partial Q_i}{\partial n} \right) \mathrm{d}s = 0, \quad i = 1, 2, \ldots, N_s. \tag{12}$$

There remains to impose the Dirichlet boundary condition along AB. To achieve that, a Lagrange multiplier function μ is employed, which replaces the normal derivative of $\bar{\Phi}$. The boundary AB is divided into N_E quadratic elements and the Lagrange multiplier function is approximated by means of quadratic basis functions P_j:

$$\bar{\mu} = \sum_{j=1}^{N_\mu} \bar{\mu}_j P_j, \tag{13}$$

where $N_\mu = 2N_E + 1$. The quadratic basis functions are also used to weigh the Dirichlet boundary condition along AB. The following linear system of equations is thus obtained:

$$\int_{\mathrm{AB}} \left(Q_i \bar{\mu} - \bar{\Phi} \frac{\partial Q_i}{\partial n} \right) \mathrm{d}s = 0, \quad i = 1, 2, \ldots, N_s \tag{14}$$

and

$$\int_{\mathrm{AB}} P_i \bar{\Phi} \mathrm{d}s = \int_{\mathrm{AB}} P_i \bar{\Phi}|_{\mathrm{AB}} \mathrm{d}s, \quad i = 1, 2, \ldots, N_\mu. \tag{15}$$

Eqs. (14) and (15) constitute a linear system of $N_s + N_\mu$ equations. This can be written in block form as follows:

$$\begin{bmatrix} \mathbf{K}_s & \mathbf{K}_\mu \\ \mathbf{K}_\mu^{\mathrm{T}} & O \end{bmatrix} \begin{bmatrix} \mathbf{X}_s \\ \mathbf{X}_\mu \end{bmatrix} = \begin{bmatrix} O \\ \mathbf{F}_\mu \end{bmatrix}, \tag{16}$$

where the left matrix is the stiffness matrix, $\mathbf{X}_s$ and $\mathbf{X}_\mu$ are the vectors of the unknown singular coefficients and Lagrange multipliers, respectively, while the right-hand-side represents a load vector. The stiffness matrix is symmetric and becomes singular when $N_s < N_\mu$.

4. Numerical results

The elements of the stiffness matrix and the load vector are calculated by means of numerical integration. Each boundary element is subdivided into 10 subintervals and a 15-point Gauss–Legendre quadrature is used over each subinterval. As already mentioned, the number of singular functions N_s should be greater than or equal to the number of Lagrange multipliers N_μ, in order to avoid ill-conditioning or singularity of the stiffness matrix. On the other hand, however, large values of N_s should be avoided because the contribution of the high-order singular functions becomes either negligible (for $r < 1$) or very large (for $r > 1$), beyond the limits double precision arithmetic can handle. Systematic runs have been carried out, in order to study the effects of both N_s and N_μ on the numerical results. Several combinations of N_s and N_μ have been tried until the optimal pair was found. After several trials, the optimal choices were found to be $N_s = 15$ and $N_\mu = 15$.

Table 1 presents the values of the first three singular coefficients calculated with $N_s = 15$ and various values of $N_\mu \leqslant N_s$. Very fast convergence is observed and very accurate values are obtained, as in previous applications of the SFBIM (e.g. [6–9]). In Table 2, the number of Lagrange multipliers is fixed to $N_\mu = 15$ and the number of singular functions is varied. It is clear that the optimal value of the latter is $N_s = 15$. Results start diverging for higher values of N_s due to the fact that the contribution of higher order terms of the solution expansion approximation become significant as the value of N_s increases after it attains a certain value. As illustrated in Table 3, the converged values of the singular coefficients, calculated with the optimal choices $N_s = 15$ and $N_\mu = 15$, are the same as the exact values up to 9 significant digits. The converged coefficients of order 3 and higher are essentially zero in agreement with the exact analytical solution. It is noted that these highly accurate results are obtained by forming and solving a linear system of just $N_s + N_\mu = 30$ equations, which highlights the very low demands of the SFBIM in processing time and computer memory.

Once the singular coefficients are estimated with sufficient accuracy and thus Φ is adequately approximated, the corresponding stresses can be calculated:

Table 1
Convergence of the approximations of the singular coefficients with N_μ; $N_s = 15$.

N_μ	$\bar{\beta}_1$	$\bar{\beta}_2$	$\bar{\beta}_3$
3	0.494033603	0.000137603	0.00000000122
5	0.499254214	0.000137854	0.00000000024
7	0.499875746	0.000138674	0.00000000011
9	0.499975388	0.000138826	0.00000000013
11	0.499993831	0.000138869	−0.00000000003
13	0.500000188	0.000138888	0.00000000000
15	0.499999999	0.000138889	0.00000000000

Table 2
Convergence of the approximations of the singular coefficients with N_s; $N_\mu = 15$.

N_s	$\bar{\beta}_1$	$\bar{\beta}_2$	$\bar{\beta}_3$
15	0.499999999	0.000138889	0.00000000000
16	0.499999120	0.000138883	0.00000000000
17	0.499997614	0.000138881	−0.00000000001
18	0.499997032	0.000138882	−0.00000000003
19	0.499994534	0.000138877	0.00000000018
20	0.499973215	0.000138794	0.00000000119
21	0.499865002	0.000137308	0.00000000184

Table 3
Converged values of the approximations of the leading singular coefficients (calculated for $N_s = N_\mu = 15$) compared against the exact analytical results.

j	$\bar{\beta}_j$	β_j
1	0.499999999	0.500000000
2	0.000138889	0.000138889
3	0.000000000	0.000000000
4	0.000000000	0.000000000
5	0.000000000	0.000000000

Table 4
Values of stresses (in kPa) and strains at the middle Λ of the curved boundary segment AB. The error is calculated as the absolute difference of the exact and approximate solutions.

	Exact solution	Approximate solution	Error
σ_{rr}	16.2006	16.2004	2×10^{-4}
$\sigma_{\theta\theta}$	−16.2006	−16.2004	2×10^{-4}
$\sigma_{r\theta}$	21.6395	21.6394	1×10^{-4}
ε_{rr}	3.0781×10^{-7}	3.0781×10^{-7}	$<10^{-12}$
$\varepsilon_{\theta\theta}$	-3.0781×10^{-7}	-3.0781×10^{-7}	$<10^{-12}$
$\varepsilon_{r\theta}$	4.1115×10^{-7}	4.1115×10^{-7}	$<10^{-12}$

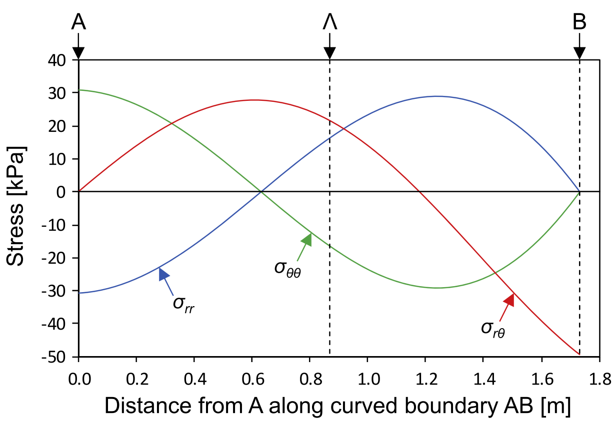

Fig. 3. Distributions of the stresses σ_{rr}, $\sigma_{\theta\theta}$ and $\sigma_{r\theta}$ along the curved boundary AB.

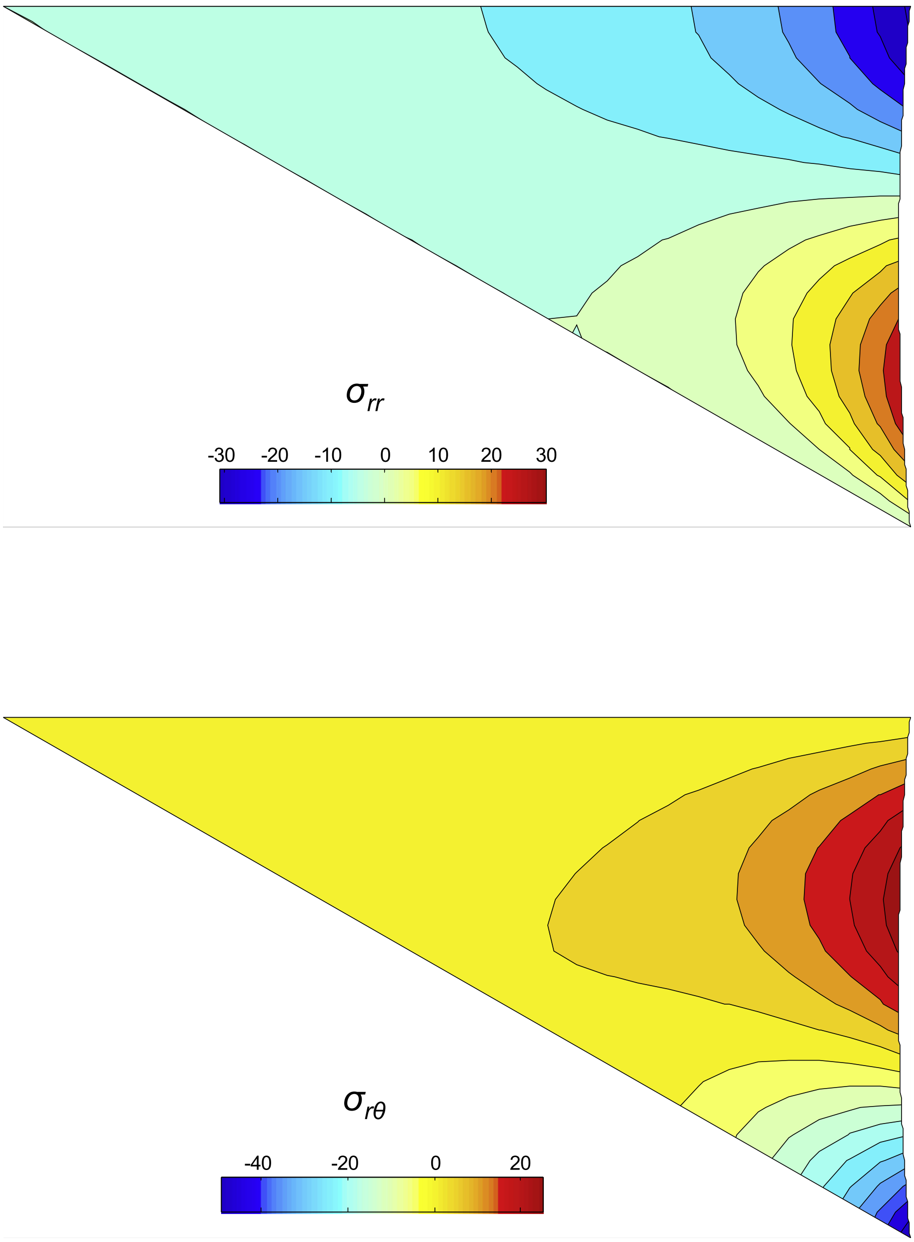

Fig. 4. Stress contours for σ_{rr} and $\sigma_{r\theta}$ (in kPa).

$$\sigma_{rr} = \frac{1}{r}\frac{\partial \Phi}{\partial r} + \frac{1}{r^2}\frac{\partial^2 \Phi}{\partial \theta^2} = -3r\cos(3\theta) - 0.01r^7\cos(9\theta), \tag{17}$$

$$\sigma_{\theta\theta} = \frac{\partial^2 \Phi}{\partial r^2} = 3r\cos(3\theta) + 0.01r^7\cos(9\theta) = -\sigma_{rr}, \tag{18}$$

$$\sigma_{r\theta} = -\frac{\partial}{\partial r}\left(\frac{1}{r}\frac{\partial \Phi}{\partial \theta}\right) = 3r\sin(3\theta) + 0.01r^7\sin(9\theta). \tag{19}$$

As shown in Table 4, the numerical values of the stresses at the middle Λ of arc AB almost coincide with the analytical ones. This is also the case with the values of strains at the same point also tabulated in Table 4. These are calculated by means of Hooke's generalized equations:

$$\varepsilon_{rr} = \frac{1}{E}(\sigma_{rr} - \nu\sigma_{\theta\theta}), \tag{20}$$

$$\varepsilon_{\theta\theta} = \frac{1}{E}(\sigma_{\theta\theta} - \nu\sigma_{rr}), \quad (21)$$

$$\varepsilon_{r\theta} = \frac{1}{2G}\sigma_{r\theta}, \quad (22)$$

where $G = E/2(1 + \nu)$ is the shear modulus of the material of the beam. The stresses of the wedge beam are graphically illustrated in Figs. 3 and 4. In particular, distributions along the curved boundary AB for all stress components are shown in Fig. 3, while contours for stresses σ_{rr} and $\sigma_{r\theta}$ over the whole analyzed domain are depicted in Fig. 4. The stress contour for $\sigma_{\theta\theta}$ is the opposite of the one for σ_{rr}, as it holds that $\sigma_{rr} + \sigma_{\theta\theta} = 0$ at any point of the analyzed domain.

5. Conclusions

In this work, the singular function boundary integral method (SFBIM) has been implemented for efficiently solving a model problem of a 2-D perfectly elastic wedge beam with a point boundary singularity and a curved boundary part. The convergence of the method has been studied by varying the numbers of singular functions and Lagrange multipliers. With the SFBIM, the leading singular coefficients of the local singularity expansion are calculated explicitly; this constitutes an important advantage over other numerical methods, which require post-processing of the solution to obtain the singular coefficients. It has been numerically demonstrated that, for the special model problem analyzed in the present paper, the SFBIM achieves fast convergence and highly accurate results.

As the complexity of the problems tackled in engineering applications is continuously increased and the resulting handling demands approach the limits of computational resources, there is a constant need for efficient and effective numerical solution methods offering both computing speed and accuracy. It is still common in engineering applications to use classical finite element software, which may offer the capability to solve many quite different problems, but may also struggle to reach an adequate solution for problems posing certain difficulties. Hence, further developing and making available numerical methods like the SFBIM is an important step towards overcoming such difficulties. Along this line, in the present work the SFBIM has been successfully applied and tested on a special model problem with non-standard boundary conditions. The demonstrated capability of the SFBIM to attain fast solutions without compromising accuracy can be a very helpful feature especially when successive linear analyses are required, e.g. in the solution of non-linear and/or dynamic problems. Efficient numerical methods like the SFBIM can be particularly useful in drastically accelerating the extremely demanding computations of reanalysis problems encountered in sensitivity analyses, Monte-Carlo simulation-based approaches, design optimization, etc.

The favorable numerical behavior of the SFBIM can be exploited also in other ways. Combining the SFBIM with standard numerical methods, such as the FEM, appears to be an interesting extension of the method. For example, Chen et al. [20] recently proposed two model order reduction techniques for Poisson singularity problems and presented the analytical investigations of accuracy and stability in the reduced models. Hence, among the future plans of the authors is to present hybrid methods simultaneously taking advantage of the strengths of the SFBIM and other numerical approaches.

References

[1] M. Elliotis, G. Georgiou, C. Xenophontos, The solution of a Laplacian problem over an L-shaped domain with a singular function boundary integral method, Commun. Numer. Methods Eng. 18 (2002) 213–222.
[2] I. Babuška, B. Guo, The *h-p* version of the finite element method – Part 1: the basic approximation results, Comput. Mech. 1 (1986) 21–41.
[3] I. Babuška, A. Miller, The post-processing approach in the finite element method – Part 1: calculation of displacements, stresses and other higher derivatives of the displacements, Int. J. Numer. Methods Eng. 20 (1984) 1085–1109.
[4] I. Babuška, A. Miller, The post-processing approach in the finite element method – Part 2: the calculation of the stress intensity factors, Int. J. Numer. Methods Eng. 20 (1984) 1111–1129.
[5] S.C. Brenner, Multigrid methods for the computation of singular solutions and stress intensity factors I: corner singularities, Math. Comput. 68 (1999) 559–583.
[6] Z.-C. Li, T.T. Lu, Singularities and treatments of elliptic boundary value problems, Math. Comput. Model. 31 (2000) 97–145.
[7] P. Grisvard, Elliptic Problems in Non-smooth Domains, Pitman Pub, England, 1985.
[8] G.C. Georgiou, L.G. Olson, W.W. Schultz, S. Sagan, A singular finite element for Stoke's flow: the stick-slip problem, Int. J. Numer. Methods Fluids 9 (1989) 1353–1367.
[9] L.G. Olson, G.C. Georgiou, W.W. Schultz, An efficient finite element method for treating singularities in Laplace's equation, J. Comput. Phys. 96 (1991) 391–410.
[10] B. Szabó, I. Babuška, Finite Element Analysis, John Wiley & Sons Inc, New York, 1991.
[11] D.M. Young, R.T. Gregory, A Survey of Numerical Mathematics, Dover Pub. Inc, New York, 1988.
[12] G.C. Georgiou, L.G. Olson, Y. Smyrlis, A singular function boundary integral method for the Laplace equation, Commun. Numer. Methods Eng. 12 (1996) 127–134.
[13] G.C. Georgiou, A. Boudouvis, A. Poullikkas, Comparison of two methods for the computation of singular solution in elliptic problems, J. Comput. Appl. Math. 79 (1997) 277–290.
[14] M. Elliotis, G. Georgiou, C. Xenophontos, Solving Laplacian problems with boundary singularities: a comparison of a singular function boundary integral method with the p/hp version of the finite element method, Appl. Math. Comput. 169 (2005) 485–499.
[15] M. Elliotis, G. Georgiou, C. Xenophontos, Solution of the planar Newtonian stick-slip problem with the singular function boundary integral method, Int. J. Numer. Methods Fluids 48 (2005) 1000–1021.
[16] M. Elliotis, G. Georgiou, C. Xenophontos, The singular function boundary integral method for a two-dimensional fracture problem, Eng. Anal. Bound. Elem. 30 (2006) 100–106.

[17] E. Christodoulou, M. Elliotis, C. Xenophontos, G. Georgiou, The singular function boundary integral method for 3-D Laplacian problems, with a boundary straight-edge singularity, Appl. Math. Comput. 219 (2012) 1073–1081.
[18] C. Xenophontos, M. Elliotis, G. Georgiou, A singular function boundary integral method for Laplacian problems with boundary singularities, SIAM J. Sci. Comput. 28 (2006) 517–532.
[19] Y.C. Fung, Foundations of Solid Mechanics, Prentice Hall Inc, New Jersey, 1977.
[20] J.-S. Chen, C. Marodon, H.-Y. Hu, Model order reduction for meshfree solution of Poisson singularity problems, Int. J. Numer. Methods Eng. (2014), http://dx.doi.org/10.1002/nme.4743.